



UDC 621.791.011

DOI 10.17073/0368-0797-2024-3-293-302



Original article

Оригинальная статья

CALCULATIONS OF PHASE COMPOSITION OF AUSTENITIC HIGH-NITROGEN WELDING WIRE AND STUDY OF A WELDED JOINT MADE FROM IT

V. S. Kostina , M. V. Kostina, D. V. Zinoveev, A. E. Kudryashov

Baikov Institute of Metallurgy and Materials Science, Russian Academy of Sciences (49 Leninskii Ave., Moscow 119991, Russian Federation)

vskostina@yandex.ru

Abstract. The processability of a material is directly related to the possibility of its production, operation and maintainability. One of the most important indicators of the processability of any metal is weldability. Austenitic steels with a high nitrogen content proved themselves as high-strength, corrosion- and cold-resistant materials, but the issue of their weldability is still not fully understood. The lack of welding filler materials on the market specifically designed for welding high-nitrogen steels is the primary obstacle to solving this problem. Thus, the goal of the work was to develop and obtain a laboratory sample of high-nitrogen welding wire. Based on calculations of nitrogen solubility and the phase composition of the weld metal, the chemical composition of Cr–Mn–Ni–Mo–V,N steel was selected for this wire. A defect-free ingot with 0.57 % N was obtained, and wire with a nitrogen content of 0.57 wt. % was produced using hot plastic deformation and drawing methods. Testing of this wire to obtain a welded joint of austenitic cast steel, close to it in chemical composition, with the welding process carried out according to the developed technological recommendations, made it possible to obtain a defect-free welded joint without loss of nitrogen in the weld metal. With a microhardness of the base metal of 252 HV₅₀, due to the alloying of the welding wire steel with nitrogen and vanadium, the metal of the weld and fusion line had a high microhardness (278 and 273 HV₅₀, respectively), significantly exceeding the microhardness of Cr–Ni cast austenite. The metal of the welded joint has high strength (0.9 of the base metal strength) and high impact toughness. The fracture of impact samples is characterized by a dimple structure characteristic of viscous materials. According to the obtained results, the new welding wire showed itself to be a promising material for welding austenitic high-nitrogen steels.

Keywords: high-nitrogen steel, welded joint, manual arc welding, high-nitrogen welding wire, mechanical properties, impact strength, fractography

Acknowledgements: The work was supported by the President, grant No. MK-1100.2022.4.

For citation: Kostina V.S., Kostina M.V., Zinoveev D.V., Kudryashov A.E. Calculations of the phase composition of austenitic high-nitrogen welding wire and study of a welded joint made from it. *Izvestiya. Ferrous Metallurgy*. 2024;67(3):293–302.

<https://doi.org/10.17073/0368-0797-2024-3-293-302>

РАСЧЕТЫ ФАЗОВОГО СОСТАВА АУСТЕНИТНОЙ ВЫСОКОАЗОТИСТОЙ СВАРОЧНОЙ ПРОВОЛОКИ И ИССЛЕДОВАНИЕ ВЫПОЛНЕННОГО ИЗ НЕЕ СВАРНОГО СОЕДИНЕНИЯ

В. С. Костина , М. В. Костина, Д. В. Зиновеев, А. Э. Кудряшов

Институт металлургии и материаловедения им. А.А. Байкова РАН (Россия, 119991, Москва, Ленинский пр., 49)

vskostina@yandex.ru

Аннотация. Технологичность материала напрямую связана с возможностью его производства, эксплуатации и ремонтпригодности. Одним из важнейших показателей технологичности металла является свариваемость. Аустенитные стали с высоким содержанием азота проявили себя как высокопрочные, коррозионно- и хладостойкие материалы, однако вопрос их свариваемости до сих пор раскрыт не до конца. Отсутствие на рынке сварочных присадочных материалов, специально разработанных для сварки высокоазотистых сталей, перво-степенная преграда перед решением обозначенной проблемы. В связи с этим целью данной работы является разработка и получение лабораторного образца высокоазотистой сварочной проволоки. На основе проведенных расчетов растворимости азота и фазового состава металла шва выбран химический состав Cr–Mn–Ni–Mo–V,N стали для этой проволоки. Получен бездефектный слиток с 0,57 % N и методами горячей пластической деформации и волочения изготовлена проволока с содержанием 0,57 мас. % N. Опробование этой проволоки для получения сварного соединения аустенитной литейной стали, близкой к ней по химическому составу, с проведением

процесса сварки по разработанным технологическим рекомендациям, позволило получить бездефектное сварное соединение без потери азота в металле шва. При микротвердости основного металла 252 HV₅₀, благодаря легированию стали сварочной проволоки азотом и ванадием металл сварного шва и линии сплавления имел высокую микротвердость (278 и 273 HV₅₀ соответственно), заметно превышающую микротвердость Cr–Ni литого аустенита. Металл сварного соединения характеризовался высокой прочностью (0,9 от прочности основного металла) и высокой ударной вязкостью. Излому ударных образцов присуще характерное для вязких материалов ямочное строение. По результатам исследования новая сварочная проволока показала себя как перспективный материал для сварки аустенитных высокоазотистых сталей.

Ключевые слова: высокоазотистая сталь, сварное соединение, ручная дуговая сварка, высокоазотистая сварочная проволока, механические свойства, ударная вязкость, фрактография

Благодарности: Работа выполнена при финансовой поддержке гранта Президента МК-1100.2022.4.

Для цитирования: Костина В.С., Костина М.В., Зиновьев Д.В., Кудряшов А.Э. Расчеты фазового состава аустенитной высокоазотистой сварочной проволоки и исследование выполненного из нее сварного соединения. *Известия вузов. Черная металлургия*. 2024;67(3):293–302. <https://doi.org/10.17073/0368-0797-2024-3-293-302>

INTRODUCTION

Due to the combination of properties, austenitic high-nitrogen steels can be used in mechanical engineering, instrumentation technology, medicine, oil and gas industry, for everyday necessities, etc. The practical application of such steels implies good processability, including weldability. While welding austenitic steels with high concentration of nitrogen (0.4 – 0.6 %), it is recommended to use the welding filler with the increased concentration of this element. It is difficult to obtain high quality welded joints of such steels as the welding filler materials developed specifically for welding high-nitrogen steels are not available in the market [1; 2]. Until recently, filler materials for welding this type of steel were chosen based on the following principles.

1. The Fe–Cr–Ni–Mo welding filler was used. In some cases, they contain small amounts of manganese and 0.10 – 0.25 % of nitrogen¹ [3; 4]. In this case, for the welding material to retain its austenitic structure, the nickel concentration in it should be significantly (~2 times) increased (compared to common stainless steels) [5; 6]. Also, for the same purpose, the carbon concentration may be slightly increased [7 – 10]. This option is most feasible in practice, but it has a number of disadvantages:

- the steel strength reduces due to the lack of solid-solution hardening with nitrogen;
- the balance shifts towards ferrite formation.

In some cases, a certain amount of nitrogen gas [11 – 14] or nitride-containing powder [15] are added to the shielding gas to increase the nitrogen content in the weld metal during welding. Addition of nitrogen in the properly calculated concentration during the welding process results in decreased ferrite amount, enhanced ductility and corrosion resistance [16 – 19].

2. Ni-based welding filler materials originally developed for welding heat-resistant steels can be used [4; 20]. They are characterized by high performance properties, but contain a large number of expensive alloying elements: 55 – 68 % Ni and 2.5 – 16 % Mo. When high-nickel fillers are used, low welding current should be applied for welding so that the high-nitrogen base metal is not mixed with the filler metal. Otherwise, the mixing zone will be depleted of nitrogen due to the high concentration of nickel, which reduces nitrogen solubility [21], thus making its zone the most vulnerable area of the welded joint [22].

3. The metal with the chemical composition similar or identical to that of the base metal can be used as the filler, this option is called autogenous TIG welding [23]. The advantage of this method is that the concentration of nitrogen in the welding filler is as high as that in the base metal, therefore, the welded joint can be expected to be quite strong. However, this option cannot be used on an industrial scale if thin base metal rods are applied for autogenous TIG welding, as many welding processes involve automatic wire feeding.

Recently, the issue of selecting welding filler materials for welding high-nitrogen steels has attracted special attention. A number of research groups have reported the development of welding wire samples with high-nitrogen content [17; 19; 24].

The authors of [24] developed three samples of experimental Cr–Mn–Ni welding wires with a nitrogen content of 0.15; 0.6 and 0.9 %. Welded joints of 22Cr–16Mn–2Ni–0.75N high-nitrogen steel were obtained using the developed wires in argon shielding gas. During the welding process, the resulting degassing of nitrogen in the molten wire droplets led to reduction in nitrogen content in the weld hard metal. As a result, some amount of ferrite was formed in the metal of welds obtained using wires with a nitrogen content of 0.6 and 0.9 %, which led to a drop in the impact strength of welded joints. At the same time, porosity was revealed in the metal of the weld with the highest nitrogen content, which negatively affected the strength of the welded

¹ https://www-eng.lbl.gov/~shuman/NEXT/MATERIALS&COMPONENTS/ss-weld_manual_avesta.pdf

joint. The welded joint with 0.15 % N had an austenitic structure, however, due to the low nitrogen concentration, its strength characteristics were the lowest.

In the study [17], welded joints of 22Cr–2Ni–16Mn–0.75N steel were obtained by arc welding using the 20Cr–2Mo–18Mn–0.6N filler. To prevent the risks of losing nitrogen from the welding wire, the Ar–N₂–CO₂ mixture was used as the shielding gas. It was found that as the CO₂ content increases, so does the nitrogen content in the weld metal, which results in enhanced strength and impact strength of the welded joint. The addition of N₂ gas (up to 7 %) also boosted the nitrogen content in the weld metal. During automatic arc welding described in [19], welded joints of 21Cr–Ni–17Mn–4Mo–0.8N steel were obtained in a shielding gas mixture of 93.5 % Ar + 5 % N₂ + 1.5 % O₂ while experimental 21Cr–2Ni–17Mn–2Mo–0.78N welding wire was used. The wire feed speed and voltage were varied. It was found that a low wire feed speed (3–8 m/min) at moderate arc voltage (up to 20 V) is preferable to ensure a stable welding process. The use of high welding speeds and higher voltages resulted in wire metal scattering and smoke in the arc burning area.

Having analyzed the reasons behind the difficulties hampering the development of a suitable high-nitrogen welding wire, we can emphasize the following. When designing a wire, it is important to take into account the chemical composition, post-weld microstructure formed by the welding wire metal and the weld crystallization mode. All of these factors can affect the wire manufacturing technology. The higher the nitrogen content of the wire metal, the more metal degassing will occur during the welding process. Accordingly, ingots obtained by smelting under nitrogen pressure are not suitable for this purpose. When developing the wire chemical composition, it is also important to take into account the content of alloying elements that tend to form hard and brittle nitrides during welding, such as Cr, Nb and V. In addition, the stacking fault energy enhances with increasing nitrogen content, which may create difficulties for welding wire drawing from steel with high nitrogen content.

Given this, the objectives of this work include developing the chemical composition of welding wire with high nitrogen content, predicting the phase composition of weld metal in Thermo-Calc, obtaining a wire laboratory sample and studying the properties of welded joints fabricated using the developed welding wire.

MATERIALS AND METHODS

As the study object, we used welded joints obtained by manual argon arc welding of austenitic steel, grade 05Kh21AG15N8MFL, with a nitrogen content of ~0.6 wt. %, 20 mm thick, in an argon environment.

After smelting, the steel was subjected to homogenizing annealing at 1200 °C for 3 h followed by cooling in water. The chemical composition of the base metal is presented in Table 1.

The welded joints were obtained based on the technological recommendations developed by the authors [25] using the following welding parameters: welding current of 100–120 A; arc voltage of 9 V; and welding speed of 3 m/h. According to the recommendations, air cooling was performed after each layer of deposited metal.

The welding wire with high nitrogen content, 1.2 mm in diameter, developed and obtained at IMET RAS was used as a welding filler material [26]. To select the chemical composition of Cr–Ni–Mn–Mo–N welding wire, we performed:

– thermodynamic calculations of nitrogen [N] solubility [27]

$$\begin{aligned} \lg[N] = & -560/T - 1,06 - 2600/T - \\ & - \{0.39(-0.048([Cr] + 0.5[Mn] - 2.45[C] - \\ & - 0.9[Si] - 0.23[Ni] + 0.27[Mo] + 2.04[V] - \\ & - 0.12[Cu] - 0.15[S] - [P] + 0.41[W]) + \\ & + 3.5 \cdot 10^{-4}([Cr] + 0.5[Mn] - 2.45[C] - \\ & - 0.9[Si] - 0.23[Ni] + 0.27[Mo] + 2.04[V] - \\ & - 0.12[Cu] - 0.15[S] - [P] + 0.41[W])^2\} + \\ & + (700/T - 0.37); \end{aligned} \quad (1)$$

– calculations of the phase composition using Schaeffler diagram based on estimated nitrogen concentrations under the following condition:

$$Ni_{eq}/Cr_{eq} > 0.8, \quad (2)$$

where the values of nickel and chromium equivalents were calculated by the following formulas

$$Ni'_{eq} = Ni + 0.1Mn - 0.01Mn^2 + 18N + 30C, \quad (3)$$

$$Cr'_{eq} = Cr + 1.5Mo + 0.48Si + 2.3V + 1.75Nb; \quad (4)$$

– ensuring corrosion resistance:

$$PREN = \% Cr + 3.3 \% Mo + 16 \% N \geq 31. \quad (5)$$

Phase composition calculations of the weld metal were performed using thermodynamic values from the TCFE 7.0 database in Thermo-Calc. The initial parameters in thermodynamic modeling were the concentrations of the system components (chemical composition), temperature and pressure. The calculations were

Table 1. Grade chemical composition of the base metal

Таблица 1. Марочный химический состав основного металла

Base metal	Chemical composition, wt. % (Fe and impurities – the rest)									
	N	Cr	Ni	Mn	Mo	Si	V	C	S	P
	maximum									
05Kh21AG15N8MFL	maximum 0.6	21 – 22	7.7 – 9.0	15 – 16	1 – 2	0.2	0.3	0.04	0.008	0.012

performed at normal atmospheric pressure in the temperature range from 600 to 1200 °C.

Fabricating the sections and revealing the microstructure. The samples were pressed into bakelite on an Opal 400 hot mounting press, then successively ground on a Saphir 250 grinder and polished on a cloth using emulsion. Polished samples of welded joints were subjected to etching in the reagent: 2 parts of HCl + 1 part of HNO₃ + 1 part of glycerin.

Optical microscopy. The microstructure was studied using an Olympus GX51 light microscope.

Ferritometry. The ferrite content was measured by the magnetometric method using an MVP-2M multifunctional eddy current tester. The ferritic phase content range can be measured from 0 to 25 %; limit of permissible basic error of the ferritic phase: $0.05(1 + X_{\phi})$, where X_{ϕ} is the measured value of the ferritic phase, %.

Microhardness. Microhardness of different zones of welded joints was measured according to GOST 9450 – 76 on a Volpert 402MVD hardness meter at a load of 50 g, with the sample being held under this load for 10 s. A tetrahedral diamond pyramid was used as an indenter. The microindentation hardness number was determined by the formula

$$HV = \frac{F}{S} = \frac{0.102 \cdot 2F \cdot \sin d/2}{d^2} = 0.189 \frac{F}{d^2}, \quad (6)$$

where F is the load, N; d is the diagonal of impression, mm.

Mechanical properties were determined on the samples of the base metal and the resulting welded joints, in which the weld was located in the center of the cut sample.

Tensile tests were conducted according to GOST 1497 – 84 on an Instron 3382 testing machine. Proportional cylindrical samples, type IV, No. 7 were used. The test was performed at a speed of 1 mm/min in all cases, at room temperature.

Impact bending tests were conducted according to GOST 9454 – 78 on an Amsler RKP 450 (Zwick/Roell) impact testing machine at 20 °C. We used the samples defined in GOST 9454 – 78 with a V -concentrator. The maximum pendulum impact energy is 300 J.

Raster electronic microscopy. Fractographic analysis of samples after destruction was carried out on a LEO-1420 scanning electron microscope with an Oxford Instruments microscope for micro X-ray spectral analysis (MXSA).

RESULTS AND DISCUSSION

Development of chemical composition and production of welding wire

The high-nitrogen welding wire was developed based on Fe–Cr–Mn steel alloyed with interstitial elements – nitrogen (~0.5 %) and carbon, substitution elements – nickel and molybdenum, which ensured an austenitic structure, high strength, corrosion and cold resistance² [4]. Based on the calculations by formulas (1) – (5) we selected the chemical composition of the welding wire (Table 2).

Due to the melting of Cr–Ni–Mn–Mo–N wires during welding, the volatile elements – nitrogen and manganese – can partially escape from the weld metal. The objective of this work is to evaluate the thermodynamically equilibrium phase composition of weld metal depending on the content of nitrogen and manganese using the Thermo-Calc software for plotting temperature sections of phase diagrams.

Fig. 1 shows the plotted phase diagrams for the composition of the new welding wire with variable nitrogen and manganese content. The dotted line indicates the amount of nitrogen and manganese contained in the weld wire metal of the calculated composition (Table 2).

In the steel of this chemical composition, in equilibrium conditions when the temperature drops to ~700 °C and nitrogen concentration decreases to 0.5 %, the undesirable Z-phase (Cr, V)N can be separated from austenite, in addition to CrN nitrides, $Me_{23}C_6$ carbides and σ -phase (Fig. 1, a). However, according to [28], the Z-phase is formed in case of long thermal soak in heat-resistant steels. Taking into account that welding is a non-equilibrium process in which each pass of the welding arc is accompanied by melting of a small area of the welded metal edge and melting of the welding wire of a small diameter

² Refer to: Ibid.

Table 2. Grade chemical composition of the welding wire metal

Таблица 2. Марочный химический состав металла сварочной проволоки

Welding wire	Chemical composition, wt. % (Fe and impurities – the rest)										[N], %	Ni _{eq} /Cr _{eq}	PREN
	N	Cr	Ni	Mn	Mo	Si	V	C	S	P			
						maximum							
Sv-0.57N	maximum 0.57	21 – 23	7.8 – 8.3	14 – 16	0.5 – 1.5	0.5	0.2	0.06	0.007	0.013	0.57	0.73	32

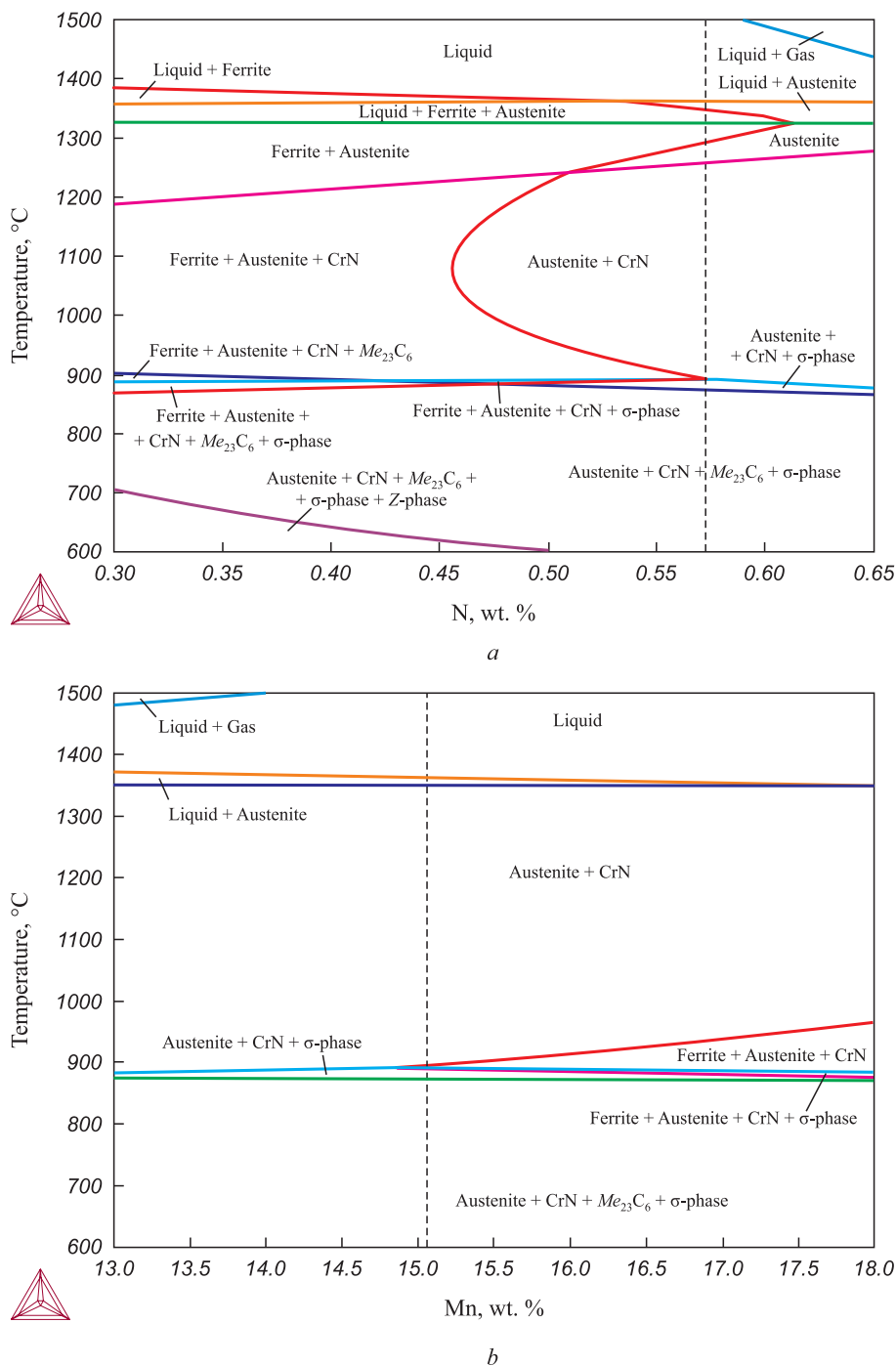


Fig. 1. Calculations of thermodynamically equilibrium phase composition of welding wire Sv-0.57N depending on the content in it of nitrogen (at 15.1 % Mn) (a) and manganese (at 0.57 % N) (b)

Рис. 1. Расчеты термодинамически равновесного фазового состава сварочной проволоки Св-0,57N в зависимости от содержания в ней азота при концентрации 15,1 % Mn (a) и марганца при концентрации 0,57 % азота (b)

(~1.2 mm), followed by cooling, undesirable Z-phase or σ -phase are not likely to emerge in the weld metal zone, fusion zone or heat affected zone of the welded product.

According to the calculated data presented in Fig. 1, *b*, some possible reduction of manganese concentration during welding cannot lead to negative changes of the phase composition, the latter should remain austenitic.

Welding wire manufacturing involved the following process steps: smelting of steel with the given chemical composition in an open induction furnace with the addition of nitrided ferroalloys; homogenization of the cast structure at 1200 °C; rolling with preheating at 1100 °C; rotary forging and wire drawing.

Microstructure

The examination in the optical light microscope did not reveal any pores, cracks or non-welds (Fig. 2). The authors of [24] present a general view of welded joints studied using the microscope of low magnification. When welding wire with 0.9 % nitrogen content was used, pores in the weld metal were observed with the naked eye.

The microstructure of the base metal, 05Kh21AG15N8MFL cast steel, is characterized by large grains of austenite, 200 – 700 μm in size (Fig. 2, *a*). The weld metal structure includes small grains elongated in the direction of crystallization (Fig. 2, *b*). A number of ferrite grains are observed in each of the weld zones. The ferritometry test revealed that the volume content of ferrite does not exceed 0.27.

Comparing the data obtained by calculations of the phase diagram presented in Fig. 1 and microstructure images, it is important to point out that optical microscopy did not confirm the presence of Me_{23}C_6 carbides and σ -phase in the obtained welded joints.

The high-temperature welding process can adversely affect the heat affected zone of the weld. Thus, for example, the works [29; 30] showed that large particles of Cr_2N nitrides were released in the heat affected zone, which led to reduction in corrosion resistance. However, large nitride particles were not detected in the studied welded joints, obviously due to the use of low weld heat input.

The nitrogen content in the weld metal amounted to 0.58 %, apparently due to the transfer of nitrogen from the base metal (with 0.6 % N) into the welding bath during welding. Such high nitrogen assimilation was achieved by following the technological recommendations for welding high-nitrogen steels [25]. In the previously discussed work [24], when multi-pass argon-arc welding and welding wires with 0.6 and 0.9 % N were used, as in this case, the nitrogen content in the weld metal was 0.54 and 0.64 %, respectively. In [17], even the addition of 5 % N_2 to the shielding gas did not help to keep all the nitrogen contained in the filler metal (0.6 %), and its value in the weld metal amounted to 0.58 %.

Mechanical properties

The weld samples for tensile and impact bending tests were cut so that the weld metal was centered on the test samples. Fig. 3 presents the histogram that demonstrates high properties in the “yield strength – tensile strength – impact strength” combination of welded joints of cast high-nitrogen steel. As a comparison, the paper [31] indicates the following mechanical properties of the 05Kh21AG15N8MFL cast steel sample after homogenization annealing at 1200 °C, 4 h: $\sigma_{0.2} = 407 \text{ MPa}$, $\sigma_u = 674 \text{ MPa}$, $KCU = 209 \text{ J/cm}^2$. Consequently, the welded joints of high-nitrogen steel investigated in this study, obtained using the developed welding material and based on the formulated technological recommendations, are practically equal in strength

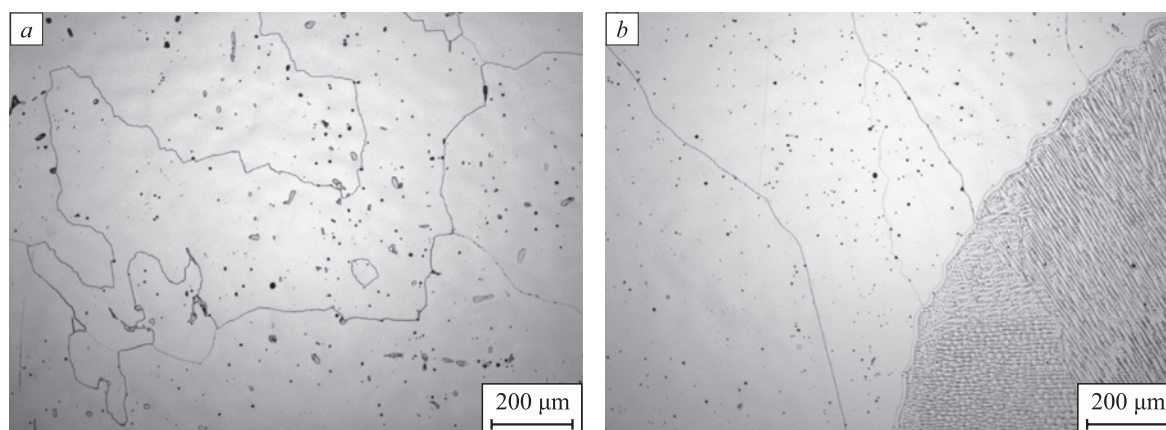


Fig. 2. Microstructure of base cast metal (*a*) and welded joint (*b*)

Рис. 2. Микроструктура основного литого металла (*a*) и сварного соединения (*b*)

to the base metal without welding (90 % of the strength of the base metal).

Microhardness values measured in different zones of the welded joint (Fig. 4) are consistent with the grain size in each of the research areas. Among other things, the lowest hardness values are typical for the base metal with the coarse-grained cast austenitic structure. The microhardness in the fusion zone and weld metal is higher as boundaries of small grains formed in the weld metal contribute to the hardening.

The fracture morphology of the samples after impact tests indicates ductile dimpled fracture pattern (Fig. 5). Large dimples contribute to enhancing plastic properties³. The steels have high impact strength when, with

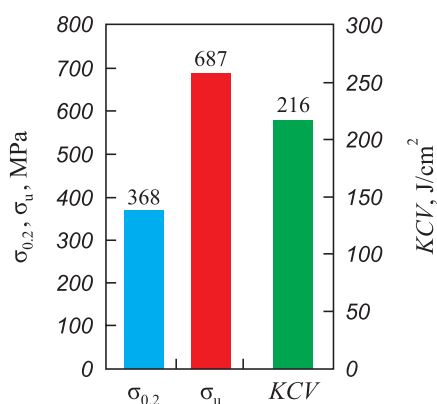


Fig. 3. Mechanical properties of the samples of welded joints of high-nitrogen austenitic steel

Рис. 3. Механические свойства образцов сварных соединений высокоазотистой аустенитной стали

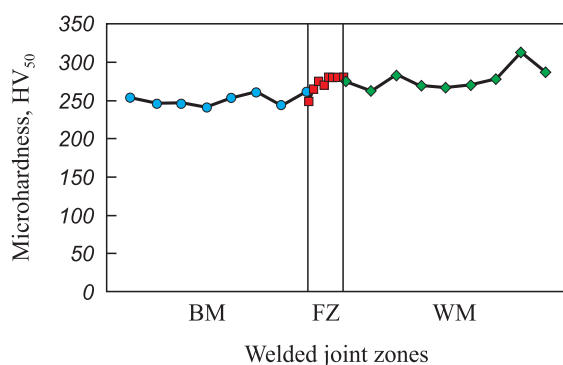


Fig. 4. Microhardness in each zone of the welded joint: BM – base metal, FZ – fusion zone, WM – weld metal

Рис. 4. Микротвердость в каждой из зон сварного соединения: BM – основной металл; FZ – зона сплавления; WM – металл шва

³ S.L. Gorobchenko, Y.S. Krivtsov, A.K. Andreev, Yu.P. Solntsev Competitiveness of reinforcement castings beyond impact strength or application of a new comprehensive method to validate the reliability of austenitic steels for cryogenic valves. TPA. Pipeline Valves & Equipment, International Magazine [Electronic resource]. URL: <http://www.valverus.info/popular/3219-konkurentosposobnost-armaturnogo-litya.html>

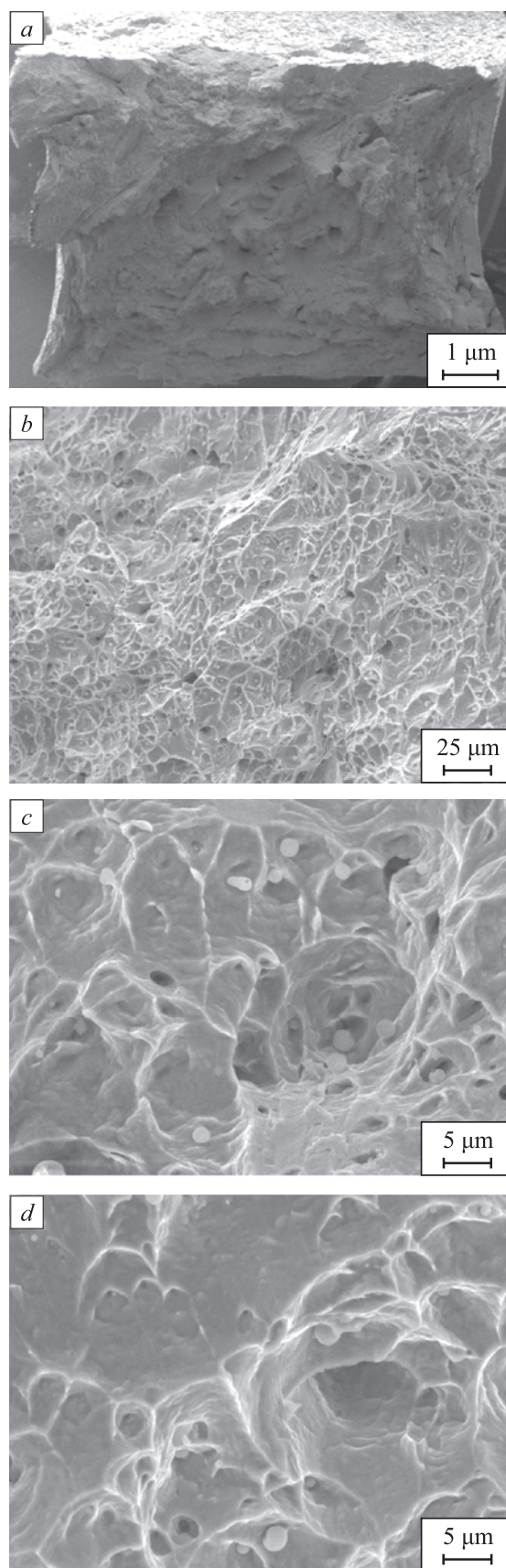


Fig. 5. Fractography of the samples of welded joints after impact tests

Рис. 5. Фрактография образцов сварных соединений после испытаний на ударную вязкость

a large number of small-sized dimples, the largest area in the fracture is covered by dimples, minimum 10 – 15 μm in size, with globular inclusions not exceeding 8 μm . Another indication of high metal ductility is the depth and plasticity of the dimples themselves, the serpentine sliding on their walls and the absence of the dimples fracturing⁴ – these are the features observed in the fracture (Fig. 5, c, d).

Discussing the strength characteristics achieved in this experiment, the following observations can be made. The strength level of a welded joint is determined by its weakest section. The authors tested this wire while welding cast austenitic steel, which is considered to be high strength among cast austenitic steels (the standard yield strength value of austenitic steels of the Fe–18Cr–10Ni system does not exceed 200 MPa). When the same wire is used for welding hot-wrought metal of the same composition, the properties of the welded joint should be higher. For example, in [24], welding filler with 0.6 % N was used to obtain a welded joint of high-nitrogen deformed steel. Accordingly, the tensile strength $\sigma_u = 912$ MPa was reached, while the impact strength was expectedly lower, $KCV = 110$ J/cm². This level of properties was obtained as the base metal structure was reinforced by deformation.

The welded joint obtained using a welding filler with 0.78 % N, during welding in the shielding gas atmosphere (87 % Ar – 6.5 % N₂ – 6.5 % CO₂), also demonstrated high mechanical properties characteristic of deformed high-nitrogen metal: $\sigma_u = 956$ MPa, $KCV = 132$ J/cm² [17].

CONCLUSIONS

We calculated the phase composition of steel of the selected composition Fe – Cr – Mn – Ni – Mo – V, N while varying the content of manganese and nitrogen, which can volatilize during welding. The study showed that the selected nitrogen-containing welding wire should have an austenitic structure.

Sv-0.57N welding wire was manufactured from the steel melted in laboratory conditions using hot plastic deformation and drawing methods. Testing of this wire to obtain a welded joint of austenitic cast steel 05Kh21AG15N8MFL ~0.6 % N, with the argon-arc welding carried out based on the developed technological recommendations, enabled to obtain a defect-free welded joint without loss of nitrogen in the weld metal.

The welded joint metal is characterized by high strength (0.9 of the base metal strength) and high impact strength, while the fracture has a dimpled structure characteristic of ductile materials. The new welding wire Sv-0.57N may be regarded as a promising material for welding austenitic high-nitrogen steels.

REFERENCES / СПИСОК ЛИТЕРАТУРЫ

1. Wang X., Tian J., Li S., He P., Fang N., Wen G. Weldability of high nitrogen steels: A review. *Reviews on Advanced Materials Science*. 2023;62(20220325):1–17. <https://doi.org/10.1515/rams-2022-0325>
2. Du Toit M. Filler metal selection for welding a high nitrogen stainless steel. *Journal of Materials Engineering and Performance*. 2002;11(3):306–312. <https://doi.org/10.1361/105994902770344123>
3. Bishokov R.V., Baryshnikov A.P., Gezha V.V., Mel'nikov P.V. Welding materials and technologies of high strength steels. *Voprosy materialovedeniya*. 2014;2(78):128–137. (In Russ.). Бишоков Р.В., Барышников А.П., Гежа В.В., Мельников П.В. Сварочные материалы и технологии сварки высокопрочных сталей. *Вопросы материаловедения*. 2014;2(78):128–137.
4. Harzenmoser M. Welding of high nitrogen steels. *Materials and Manufacturing Processes*. 2004;19(1):75–86. <https://doi.org/10.1081/AMP-120027503>
5. Du Toit M. The microstructure and mechanical properties of Cromanite welds. *Journal of the South African Institute of Mining and Metallurgy*. 1999;99(6):333–339.
6. Mohammed R., Reddy G.M., Rao K.S. Effect of filler wire composition on microstructure and pitting corrosion of nickel free high nitrogen stainless steel GTA welds. *Transactions of the Indian Institute of Metals*. 2016;69(10):1919–1927. <https://doi.org/10.1007/s12666-016-0851-6>
7. Fomina O.V. Creation of technological principles for controlling the structure and physical and mechanical properties of high-strength austenitic nitrogen-containing steel: Dr. Tech. Sci. Diss. St. Petersburg; 2018:433. (In Russ.). Фомина О.В. Создание технологических принципов управления структурой и физико-механическими свойствами высокопрочной аустенитной азотсодержащей стали: Диссертация ... доктора технических наук. Санкт-Петербург; 2018:433.
8. Mohammed R., Madhusudhan R.G., Rao K.S. Welding of nickel free high nitrogen stainless steel: Microstructure and mechanical properties. *Defence Technology*. 2017;13:59–71. <https://doi.org/10.1016/j.dt.2016.06.003>
9. Liu Z., Fan C., Yang C., Zhu Ming, Hua Z., Lin S., Wang L. Investigation of the weldability of dissimilar joint between high nitrogen steel and low alloy steel by comparing filler metals. *Materials Today Communications*. 2023;35:105551. <https://doi.org/10.1016/j.mtcomm.2023.105551>
10. Kumar N., Arora N., Goel S.K., Goel D.B. A comparative study of microstructure and mechanical properties of 21-4-N steel weld joints using different filler materials. *Materials Today Proceedings*. 2018;5(9):17089–17096. <https://doi.org/10.1016/j.matpr.2018.04.116>
11. Kokawa H. Nitrogen absorption and desorption by steels during arc and laser welding. *Welding International*. 2004;18(4):277–287. <https://doi.org/10.1533/wint.2004.3235>
12. Du Toit M., Pistorius P.C. Nitrogen control during the auto-genous ARC welding of stainless steel. *Welding in the World*. 2003;47(9–10):30–43. <https://doi.org/10.1007/BF03266398>
13. Huang H.-Y. Effects of shielding gas composition and activating flux on GTAW weldments. *Materials & Design*. 2009;30(7):2404–2409. <https://doi.org/10.1016/j.matdes.2008.10.024>
14. Kah P., Martikainen J. Influence of shielding gases in the welding of metals. *The International Journal of Advanced*

⁴ Refer to: Ibid.

- Manufacturing Technology*. 2013;64:1411–1421.
<https://doi.org/10.1007/s00170-012-4111-6>
15. Liu Z., Fan C., Chen C., Ming Z., Liu A., Yang C., Lin S., Wang L. Optimization of the microstructure and mechanical properties of the high nitrogen stainless steel weld by adding nitrides to the molten pool. *Journal of Manufacturing Processes*. 2020; 49:355–364.
<https://doi.org/10.1016/j.jmapro.2019.12.017>
 16. Zhao L., Tian Z., Peng Y., Qi Y., Wang Y. Influence of nitrogen and heat input on weld metal of gas tungsten arc welded high nitrogen steel. *Journal of Iron and Steel Research, International*. 2007;14(5):259–262.
[https://doi.org/10.1016/S1006-706X\(08\)60090-4](https://doi.org/10.1016/S1006-706X(08)60090-4)
 17. Liu Z., Fan C., Ming Z., Chen C., Yang C., Lin S., Wang L. Optimization of shielding gas composition in high nitrogen stainless steel gas metal arc welding. *Journal of Manufacturing Processes*. 2020;58:19–29.
<https://doi.org/10.1016/j.jmapro.2020.08.001>
 18. Qiang W., Wang K. Shielding gas effects on double-sided synchronous autogenous GTA weldability of high nitrogen austenitic stainless steel. *Journal of Manufacturing Processes*. 2017; 250:169–181. <https://doi.org/10.1016/j.jmatprotec.2017.07.021>
 19. Yang D., Xiong H., Huang Y., Yan D., Li D., Peng Y., Wang K. Droplet transfer behavior and weld formation of gas metal arc welding for high nitrogen austenitic stainless steel. *Journal of Manufacturing Processes*. 2021;65:491–501. <https://doi.org/10.1016/j.jmapro.2021.03.048>
 20. Zhang Y., Jing H., Xu L., Han Y., Zhao L., Xiao B. Microstructure and mechanical performance of welded joint between a novel heat-resistant steel and Inconel 617 weld metal. *Materials Characterization*. 2018;139:279–292.
<https://doi.org/10.1016/j.matchar.2018.03.012>
 21. Pehlke R.D., Elliott J.F. Solubility of nitrogen in liquid iron alloys. *Transactions of the Metallurgical Society of AIME*. 1960;218(6):1088–1101.
 22. Bonnefois B., Coudreuse L., Charles J. A-TIG welding of high nitrogen alloyed stainless steels: a metallurgically high-performance welding process. *Welding International*. 2004;18(3):208–212. <https://doi.org/10.1533/wint.2004.3226>
 23. Bannykh O.A., Blinov V.M., Kostina M.V., Blinov E.V., Zvereva T.N. Study of the weldability of high-nitrogen corrosion-resistant austenitic steels of the X22AG16N8M type. *Metally*. 2007;(4):51–67. (In Russ.).
Баных О.А., Блинов В.М., Костина М.В., Блинов Е.В., Зверева Т.Н. Исследование свариваемости высокоазотистых коррозионностойких аустенитных сталей типа X22AG16N8M. *Металлы*. 2007;(4):51–67.
 24. Liu Z., Fan C., Chen C., Ming Z., Yang C., Lin S., Wang L. Design and evaluation of nitrogen-rich welding wires for high nitrogen stainless steel. *Journal of Materials Processing Technology*. 2021;288:116885.
<https://doi.org/10.1016/j.jmatprotec.2020.116885>
 25. Kostina V.S. Research and development of technological fundamentals for welding high-nitrogen corrosion-resistant Cr-Ni-Mn-Mo austenitic steels: Cand. Tech. Sci. Diss. Moscow: IMET RAS; 2020:181. (In Russ.).
Костина В.С. Исследование и развитие технологических основ сварки высокоазотистых коррозионностойких Cr-Ni-Mn-Mo аустенитных сталей: Диссертация ... кандидата технических наук. Москва: ИМЕТ РАН; 2020:181.
 26. Kostina V.S., Kostina M.V., Dormidontov N.A., Muradyan S.O. Welding wire with high nitrogen content. Patent for invention 2768949 C1, 25.03.2022. Application No. 2021110801 dated 16.04.2021. Publ. 25.03.2022. (In Russ.).
Сварочная проволока с высоким содержанием азота. Костина В.С., Костина М.В., Дормидонтов Н.А., Мурадян С.О. / Патент на изобретение 2768949 C1, 25.03.2022. Заявка № 2021110801 от 16.04.2021. Дата публикации: 25.03.2022.
 27. Rigina L.G., Vasiliev Ya.M., Dub V.S., etc. Alloying steel with nitrogen. *Elektrometallurgiya*. 2005;(2):14–21. (In Russ.).
Ригина Л.Г., Васильев Я.М., Дуб В.С. и др. Легирование стали азотом. *Электрометаллургия*. 2005;(2):14–21.
 28. Mohammed R., Reddy G.M., Rao K.S. Microstructure and pitting corrosion of shielded metal arc welded high nitrogen stainless steel. *Defence Technology*. 2015;11(3):237–243.
<https://doi.org/10.1016/j.dt.2015.04.002>
 29. Ogawa M., Hiraoka K., Katada Y., Sagara M., Tsukamoto S. Chromium nitride precipitation behavior in weld heat-affected zone of high nitrogen stainless steel. *ISIJ International*. 2002;42(12):1391–1398.
<https://doi.org/10.2355/isijinternational.42.1391>
 30. Moon J., Ha H.-Y., Lee T.-H., Lee C. Different aspect of pitting corrosion and interphase corrosion in the weld heat-affected zone of high-nitrogen Fe-18Cr-10Mn-N steel. *Materials Chemistry and Physics*. 2013;142(2-3):556–563.
<https://doi.org/10.1016/j.matchemphys.2013.07.052>
 31. Muradyan S.O. Structure and properties of casting corrosion-resistant steel alloyed with nitrogen: Cand. Tech. Sci. Diss. Moscow; 2016:132. (In Russ.).
Мурадян С.О. Структура и свойства литейной коррозионностойкой стали, легированной азотом: Диссертация ... кандидата технических наук. Москва; 2016:132.

Information about the Authors

Сведения об авторах

Valentina S. Kostina, Cand. Sci. (Eng.), Junior Researcher of the Laboratory "Physicochemistry and Mechanics of Metallic Materials", Baikov Institute of Metallurgy and Materials Science, Russian Academy of Sciences

ORCID: 0000-0001-7956-499X

E-mail: vskostina@yandex.ru

Mariya V. Kostina, Dr. Sci. (Eng.), Assist. Prof., Senior Researcher, Head of the Laboratory "Physicochemistry and Mechanics of Metallic Materials", Baikov Institute of Metallurgy and Materials Science, Russian Academy of Sciences

ORCID: 0000-0002-2136-5792

E-mail: mvk@imet.ac.ru

Валентина Сергеевна Костина, к.т.н., младший научный сотрудник лаборатории физикохимии и механики металлических материалов, Институт металлургии и материаловедения им. А.А. Байкова РАН

ORCID: 0000-0001-7956-499X

E-mail: vskostina@yandex.ru

Мария Владимировна Костина, д.т.н., доцент, ведущий научный сотрудник, заведующий лабораторией физикохимии и механики металлических материалов, Институт металлургии и материаловедения им. А.А. Байкова РАН

ORCID: 0000-0002-2136-5792

E-mail: mvk@imet.ac.ru

Dmitrii V. Zinoveev, Cand. Sci. (Eng.), Junior Researcher of the Laboratory "Physicochemistry and Technology of Iron Ore Processing", Baikov Institute of Metallurgy and Materials Science, Russian Academy of Sciences

ORCID: 0000-0003-4520-4659

E-mail: zinoveevimet@yandex.ru

Aleksandr E. Kudryashov, Research Engineer, Baikov Institute of Metallurgy and Materials Science, Russian Academy of Sciences

E-mail: al.kudriashov@mail.ru

Дмитрий Викторович Зиновеев, к.т.н., младший научный сотрудник лаборатории физикохимии и технологии переработки железорудного сырья, Институт металлургии и материаловедения им. А.А. Байкова РАН

ORCID: 0000-0003-4520-4659

E-mail: zinoveevimet@yandex.ru

Александр Эдуардович Кудряшов, инженер-исследователь, Институт металлургии и материаловедения им. А.А. Байкова РАН

E-mail: al.kudriashov@mail.ru

Contribution of the Authors

V. S. Kostina – conducting the research, writing the text, processing the results.

M. V. Kostina – finalization of the text, correction of conclusions.

D. V. Zinoveev – carrying out calculations of the phase composition.

A. E. Kudryashov – study of the structure of welded joints.

Received 14.12.2023

Revised 18.01.2024

Accepted 28.02.2024

Вклад авторов

В. С. Костина – проведение исследований, подготовка текста статьи, обработка результатов.

М. В. Костина – доработка текста, корректировка выводов.

Д. В. Зиновеев – проведение расчетов фазового состава.

А. Э. Кудряшов – исследование структуры сварных соединений.

Поступила в редакцию 14.12.2023

После доработки 18.01.2024

Принята к публикации 28.02.2024